

# Effects of low temperatures, low pressures and seeding over the crystalline quality, yield and stress of diamond films grown by ECR-assisted chemical vapor deposition

S. GUPTA, G. MORELL, R. S. KATIYAR  
*University of Puerto Rico, San Juan, PR 00931, USA*

D. R. GILBERT, R. K. SINGH  
*University of Florida, Gainesville, FL 32611, USA*  
*E-mail: gmorell@rrpac.upr.clu.edu*

We have studied diamond films grown by electron cyclotron resonance (ECR)-assisted chemical vapor deposition (CVD) on Si (100) substrates seeded with diamond, boron nitride and unseeded. Relatively low temperatures (550–710°C) and low pressures (1–2 Torr) were employed. Raman spectroscopy, scanning electron microscopy (SEM), and X-ray diffraction (XRD) were used to characterize the crystalline quality, diamond yield, and stresses developed in these films. Most of the diamond films exhibit a Raman blue-shift with respect to natural diamond, indicating that the net stress is compressive. However, this net stress is significantly more compressive than the one estimated by taking into account the thermal interfacial stress and the stress developed at the grain boundaries. In addition, this net stress exhibits an inverse correlation with diamond yield, and a direct correlation with crystalline quality. These results were interpreted in terms of the critical interplay between the supply of precursor species to the growing surface and the surface mobility of adsorbed species. The excess (or intrinsic) compressive stress shows an inverse correlation with diamond crystalline quality, indicating that the creation of point defects serves as a stress-relieving mechanism. Seeding effects, in general, are deleterious to diamond quality, in this temperature and pressure regime studied. Seeding with boron nitride had the effect of reversing the net stress from compressive into tensile, but this effect was rapidly lost as the diamond yield increased. © 2000 Kluwer Academic Publishers

## 1. Introduction

Diamond is a promising material for optical and electronic applications in high temperature/high power electronics, high microwave power transmission, device miniaturization and flat panel displays. This usefulness of diamond stems from its extreme hardness combined with chemical inertness and wide spectral transparency. Considerable efforts are currently devoted to understand and control the nature and sources of stresses that develop during diamond film growth since they affect substantially its physical properties [1]. In this report, we analyze the effects of relatively low temperatures (550–710°C) and pressures (1–2 Torr), and of seeding over the properties of diamond films grown by Electron Cyclotron Resonance (ECR) assisted Chemical Vapor Deposition (CVD). We employed Raman spectroscopy, X-ray diffraction (XRD), and scanning electron microscopy (SEM) to evaluate the degree of crystallinity, diamond content, intrinsic and residual stresses, surface morphology, and average grain size. The results from these nondestructive

techniques as a function of growth conditions were used to elucidate the sources of stress and to assess the role of seeding in its modification. The correlations found among diamond crystalline quality, diamond yield and stress can be explained in terms of the critical interplay between the supply of precursor species and the surface mobilities for the relatively low pressures and temperatures employed in this study.

## 2. Experimental details

The diamond films were prepared by Electron Cyclotron Resonance (ECR) Chemical Vapor Deposition (CVD) technique. The details of the preparation technique are described elsewhere [2, 3]. Here, we summarize them briefly. The diamond film growth was performed on Si (100) substrates at temperatures ranging from 550–710°C, while the pressures ranged between 1–2 Torr. Methane (CH<sub>4</sub>) was employed as carbon source under high hydrogen (H<sub>2</sub>) gas dilution (99%). The total flow rate was kept at 100 sccm for all samples.

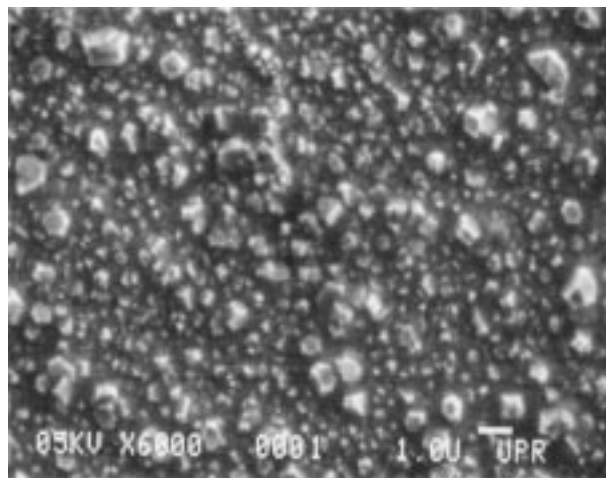
Deposition was carried out for 5 hours, resulting in films of around 1  $\mu\text{m}$  thick.

The micro-Raman spectra were obtained with a T64000 (Jobin-Yvon, ISA) triple grating spectrometer in the subtractive mode. The measurements were performed in the backscattering configuration, using the 514.5 nm line of an Ar<sup>+</sup> laser (Coherent Innova 90 Plus) as an excitation source with 10 mW incident power (around 5  $\mu\text{m}$  beam spot size). The spectrometer slits were set at 100  $\mu\text{m}$ , resulting in a resolution of 1.0  $\text{cm}^{-1}$  and uncertainties of 0.3  $\text{cm}^{-1}$  in peak positions. In order to obtain the maximum information from the Raman spectra, we recorded both the parallel  $Z(XX)\bar{Z}$  and perpendicular  $Z(XY)\bar{Z}$  components of the Raman scattering for each particular sample area. These components were then combined into a single characteristic spectrum of the film under study. This is since the true characteristic spectrum of any diamond film is the sum of these two orthogonal spectra [4, 5]. Moreover, for extracting the intrinsic Raman bandwidth we employed a mathematical simulation procedure that allows the separation of the instrumental contribution [6–8]. The diamond purity was evaluated from the ratio of the diamond peak area to that of the rest of the spectrum between 1100–1700  $\text{cm}^{-1}$  (taking the Raman scattering cross-section of non-sp<sup>3</sup> bonded carbon to be 50 times that of diamond) [9].

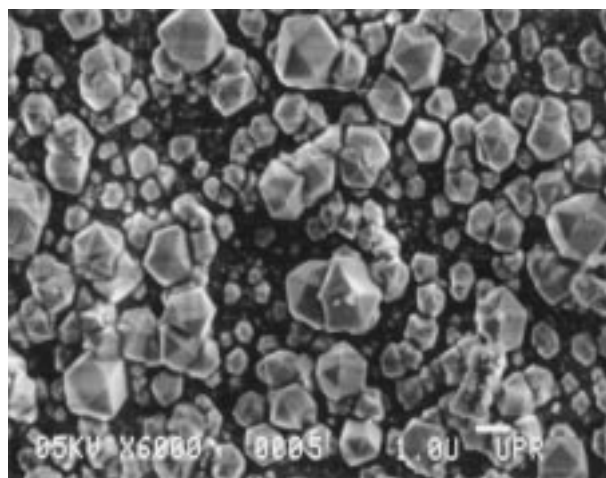
The average grain sizes were estimated from SEM (JEOL 35, CF), while the size of the coherently diffracting domains (CDD) [1] contained within each grain was calculated by deconvolution of the diffraction peak breadth [10, 11] where the XRD measurements were taken by Siemens D5000 diffractometer using a Cu-K $\alpha$  line source.

### 3. Results and discussion

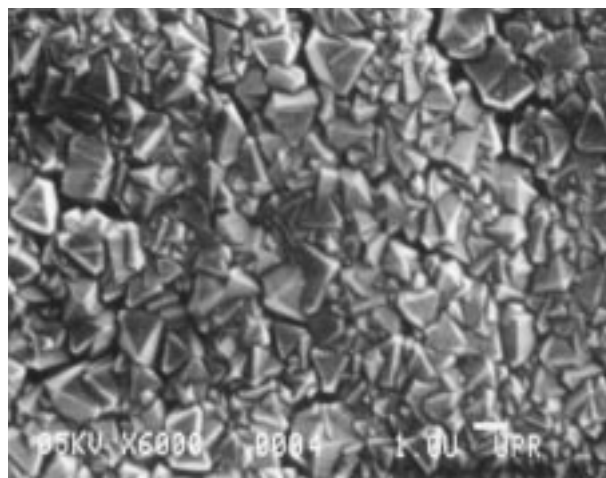
The diamond films hereby studied were grown by ECR-assisted CVD under varying conditions of substrate temperature, pressure, and seeding. These films showed variations in their crystallite size and morphology as seen in the SEM micrographs (Fig. 1), in their bandwidth, position and area ratios of the Raman peaks (Fig. 2), and in the integral width of their XRD peaks (Fig. 3). The crystallite sizes measured from the SEM pictures (Fig. 1) ranged between 0.5 and 2  $\mu\text{m}$ , with preferentially square morphology in the unseeded films, triangular in the diamond-seeded films, and hexagonal in the boron nitride-seeded films. Larger crystallite sizes were associated to seeding, with either diamond or boron nitride (BN), as expected. The diamond Raman bandwidths (Fig. 2) ranged between 4 and 10  $\text{cm}^{-1}$ , after correcting for the instrumental contribution, and therefore broad compared to that of natural diamond (i.e.,  $\approx 1 \text{ cm}^{-1}$ ). Together with this band broadening, Raman blue-shifts with respect to natural diamond (1332.5  $\text{cm}^{-1}$ ) of up to 1.4  $\text{cm}^{-1}$  were found in all except one sample, indicating the existence of net compressive stresses of up to 2.7 GPa [12]. From the Raman spectra it was also possible to estimate the diamond yield by taking the ratio of the diamond to non-sp<sup>3</sup> areas, after accounting for the difference in Raman cross-sections [9]. The calculated diamond yields var-



(a)



(b)



(c)

Figure 1 Scanning electron micrographs of (a) unseeded, (b) boron nitride, and (c) diamond seeded diamond films. The white bar corresponds to 1.0  $\mu\text{m}$ .

ied between 50–95%, for the growth parameters employed in this study. The X-ray diffractograms (Fig. 3) show the (111) and (220) peaks of diamond, for all the samples. In addition, they show a SiC diffraction peak, indicating the existence of a SiC interlayer. The prominent Si diffraction peak is due to the substrate. From the diffraction peak positions it was determined that the diamond lattice constant of our films is about 1% smaller than that of natural diamond, in agreement with the

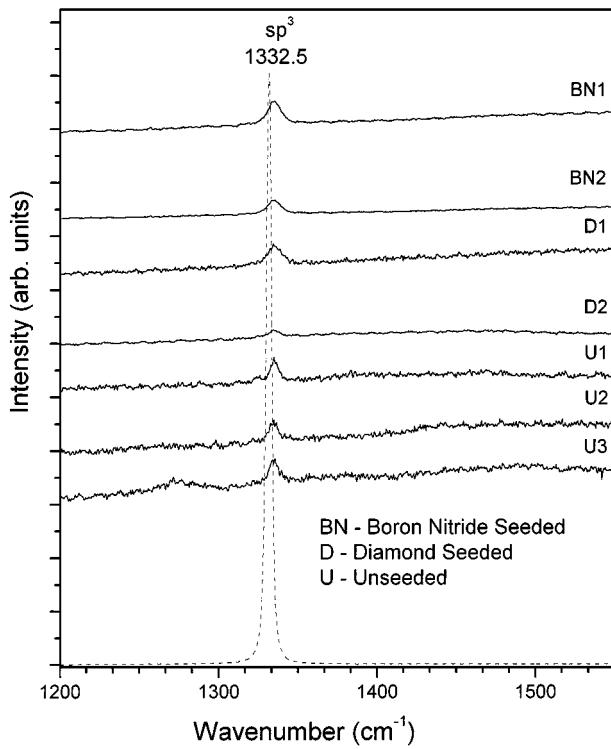


Figure 2 Raman spectra of the seven diamond films. The Raman spectrum of natural diamond (dotted line) is also shown for comparison.

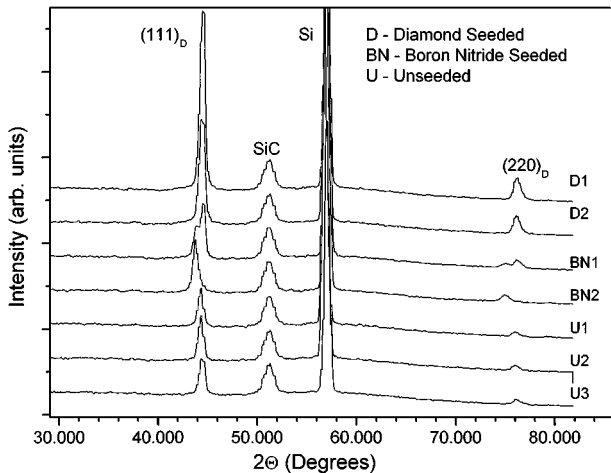


Figure 3 X-ray diffraction spectra of the seven diamond films.

net compressive stress indicated by the corresponding Raman blue-shifts. From the diffraction data, we also calculated the average size of the coherently diffracting domains (CDD) [1] within our diamond crystallites. They were found to be around 260 Å in the direction perpendicular to the (111) planes and around 150 Å in the direction perpendicular to the (220) planes. These CDDs are much smaller than the crystallite sizes judged from the SEM pictures, thus indicating that  $\mu\text{m}$ -scale grains have many internal surfaces and/or cracks.

In the low pressure and temperature regime hereby studied, increasing the temperature by 150 °C resulted in a diamond yield increment from 58 to 72%, as shown in Fig. 4. An increase in Raman bandwidth and, thus, a decrease in diamond crystalline quality accompanies this improved diamond yield. This is since phonon lifetime is inversely proportional to bandwidth and crys-

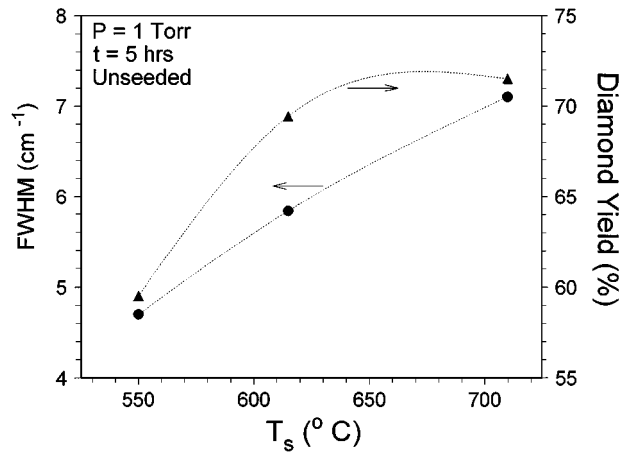


Figure 4 Correlation of substrate temperature ( $T_s$ ) with Raman bandwidth (FWHM) and diamond yield for the unseeded diamond films. Dotted lines are drawn to guide the eye.

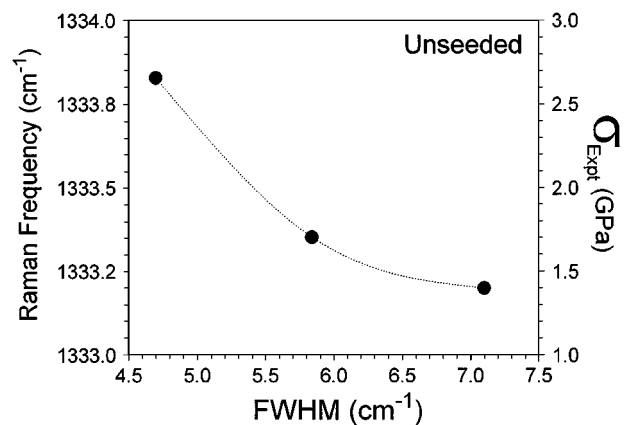


Figure 5 Correlation of Raman bandwidth (FWHM) with Raman frequency and experimental total stress ( $\sigma_{\text{exp}}$ ) for the unseeded diamond films. Dotted line is drawn to guide the eye.

talline defects diminish phonon lifetimes. Therefore, there is a fundamental trade-off between diamond yield and quality for the experimental parameters employed.

There is a particularly interesting relationship between Raman bandwidths and Raman frequencies, shown in Fig. 5. The narrower the Raman bandwidths, the larger the corresponding blue-shifts. These blue-shifts are directly related to the net stress in the films by the pressure coefficient of 1.9  $\text{cm}^{-1}/\text{GPa}$  [12]. Thus, the better the crystallinity of our diamond films the higher their stress. In order to understand this result, it is necessary to take into account that these films were grown at relatively low pressures and temperatures. The fact that there is a window in parameter space for diamond growth means that the fundamental diamond deposition process is a delicate balance between the supply of precursors from the gas phase into the growing surface and the proper positioning of these precursors within the growing lattice. Our films were grown near the edge of this parameter window, thus they give the opportunity to assess this interplay between the surface mobilities and the supply of precursor species from the gas phase. In this context, the inverse relationship between stress and crystalline quality (Fig. 5) can be ascribed to a short supply of precursor species associated

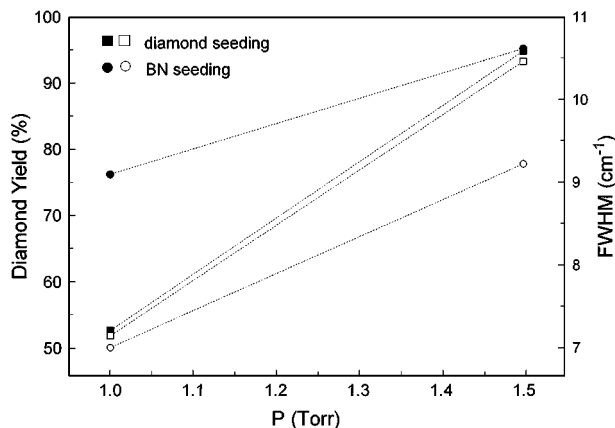


Figure 6 Effect of pressure increment over diamond yield and Raman bandwidth (FWHM) for the seeded (BN and diamond) diamond films. Filled symbols correspond to samples grown at 710 °C, while open symbols correspond to films grown at 550 °C. Dotted lines are drawn to guide the eye.

to the low growing pressures. As the growing temperature increases, the fraction of open sites increases and surface mobilities improve, causing an improvement in diamond yield (Fig. 4). However, the low pressures employed maintain a limited supply of precursor species to the growing surface, thus facilitating the formation of point defects such as empty sites. This mechanism relieves the stress and results in high defect densities.

Seeding the substrate with either diamond or boron nitride results in broader Raman bandwidths (Fig. 6) and, thus, poorer crystalline quality. No increment is observed in diamond yield upon seeding for samples grown at 1.0 Torr, when compared to the unseeded ones (Fig. 4). However, a large increment in diamond yield occurred when the pressure was increased from 1.0 to 1.5 Torr for the seeded samples (Fig. 6). This result supports the previous explanation that at a pressure of 1.0 Torr the small supply of precursor species to the growing surface is the limiting step, thus causing the diamond to grow with a high defect density when surface mobilities were improved (Fig. 4). Regarding the total stress, BN seeding had the effect of turning it tensile instead of compressive (see Table I). However, as the diamond yield increased by increasing the deposition pressure, this effect over the total stress is lost. This is expected, since after a few diamond layers are deposited, the substrate effect becomes less important.

Estimated net stresses (see Table I) that were obtained by taking into account the grain boundary component

TABLE I Experimental and calculated stress components of the seven diamond films, and the corresponding estimated excess stresses ( $\Delta$ )

Sample Id	$\sigma_{\text{Expt}}$ (GPa)	$\sigma_{\text{Th}}$ (GPa)	$\sigma_{\text{GB}}$ (GPa)	$\sigma_{\text{Calc}}$ (GPa) = $\sigma_{\text{Th}} + \sigma_{\text{GB}}$	$\Delta$ (GPa) = $\sigma_{\text{Expt}} - \sigma_{\text{Calc}}$
U1	-2.66	-0.60	+0.41	-0.19	-2.47
U2	-1.41	-0.60	+0.21	-0.39	-1.02
U3	-1.71	-0.60	+0.21	-0.39	-1.32
D1	-2.32	-0.60	+0.05	-0.55	-1.77
D2	-2.20	-0.60	+0.10	-0.50	-1.70
BN1	-1.84	-0.60	+0.05	-0.55	-2.19
BN2	+2.72	-0.60	+0.07	-0.53	+2.19

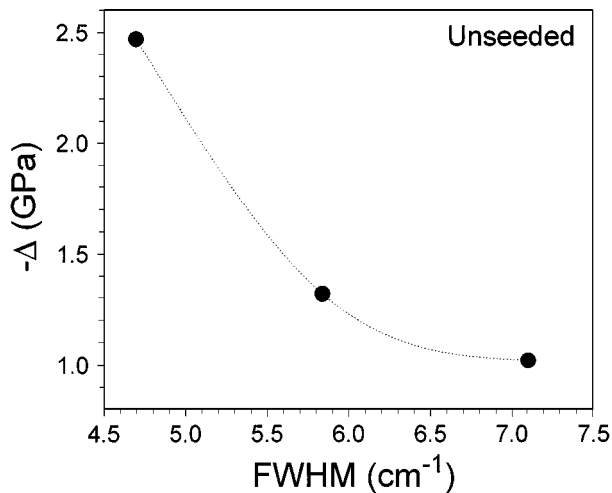


Figure 7 Correlation between the Raman bandwidth (FWHM) and estimated excess internal stress ( $\Delta$ ). Dotted line is drawn to guide the eye.

[10, 11] and the maximum thermal stress component [1, 13] give net compressive stresses in the range of 0.2 to 0.5 GPa. These calculated stresses remain between 1.0 and 2.5 GPa below the corresponding net compressive stresses derived from the Raman blue-shifts. Such a discrepancy cannot be accounted for by the phonon confinement effect, since the calculated CDD sizes are larger than 10 nm, which is the threshold for confinement effects to start showing [12]. In addition, the simulations performed on the Raman spectra did not give any indication of confinement effects or any other band-distorting effect such as degeneracy lifting, which would have required overlapping bands to properly account for the observed band shapes. Therefore, the Raman blue-shifts are just showing the total stress. It is then possible to calculate the magnitude of the excess (or intrinsic) stress (see  $\Delta$  in Table I) [12]. An inverse relationship is found between the excess stress ( $\Delta$ ) and Raman bandwidth (FWHM), that is depicted in Fig. 7. This result can be understood as indicating that the excess stress ( $\Delta$ ) showing up in the Raman blue-shift stems from strained  $sp^3$  bond-lengths resulting from the low mobilities. This strain becomes relieved by the creation of point defects, which then shows up as Raman band broadening.

#### 4. Summary

Raman spectroscopy, scanning electron microscopy (SEM), and X-ray diffraction (XRD) were employed to investigate the crystalline quality, diamond yield, and stresses developed in ECR-assisted CVD diamond films. Films were either unseeded or seeded (with BN or diamond), and relatively low temperatures and pressures were employed. It was found that there is a fundamental trade-off between diamond yield and quality. There is also an inverse relationship between stress and crystalline quality that can be ascribed to a stress-relieving mechanism, which results in high defect densities. No increment was observed in diamond yield upon seeding. However, a large increment in diamond yield occurred upon pressure increase. This was understood as indicating that the short supply of precursor

species to the growing surface was the limiting step. Boron nitride seeding had the effect of turning the net stress from compressive into tensile, but this effect was lost as the diamond yield increased. There is also an inverse relationship between the excess stress ( $\Delta$ ) and Raman bandwidth (FWHM), that was taken as an indication that in this low pressure and temperature regime, intrinsic stress stemming from low mobilities gets relieved by creation of point defects.

### Acknowledgements

This work was co-sponsored by U.S. National Science Foundation Grant No. NSF-OSR-9452893, DOD ONR Grant No. N00014-98-1-0570, DOE Grant No. DE-FG02-99ER45796 and UPR FIPI Grant No. 880244.

### References

1. D. RATS, L. BIMBAULT, L. VENDENBULCKE, R. HERBIN and K. F. BADAWI, *J. Appl. Phys.* **78** (1995) 4994.
2. R. K. SINGH, D. R. GILBERT, J. FITZ-GERALD, S. HARKNESS and D. G. LEE, *Science* **272** (1996) 396.

3. R. K. SINGH and D. R. GILBERT, *J. Mater. Res.* **4** (1998) 385.
4. G. MORELL, O. QUIÑONES, Y. DÍAZ, I. M. VARGAS, B. R. WEINER and R. S. KATIYAR, *Diamond and Related Materials* **7** (1998) 1029.
5. R. E. SHRODER, R. J. NEMANICH and J. T. GLASS, *SPIE. Diamonds Optics, B* **969** (1988) 79.
6. G. MORELL, W. PÉREZ, E. CHING-PRADO and R. S. KATIYAR, *Phys. Rev. B* **53** (1996) 5388.
7. D. W. MARQUARDT, *J. Soc. Indust. Appl. Math.* **11** (1963) 431.
8. K. LEVENBERG, *Quart. Appl. Phys. Lett.* **65** (1994) 1641.
9. R. C. HYER, M. GREEN and S. C. SHARMA, *Phys. Rev. B* **49** (1994) 14573.
10. B. QU, D. KONG, W. ZHONG, P. ZHANG and Z. WANG, *Ferroelectrics* **145** (1993) 39.
11. B. D. CULLITY, in "Elements of X-ray Diffraction" (Addison-Wesley Pub Co., 1967) p. 262.
12. L. BERGMAN and R. J. NEMANICH, *J. Appl. Phys.* **78** (1995) 6709.
13. L. SHAFER, X. JIANG and C. P. KLAGES, in "Applications of Diamond and Related Materials," edited by Y. Tzang, M. Yoshikawa, M. Murakawa and A. Feldmann (Elsevier, Amsterdam, 1991) p. 121.

*Received 18 January 1999  
and accepted 11 April 2000*